

# Antiadhesive Effects of GRN163L—An Oligonucleotide N3'→P5' Thio-Phosphoramidate Targeting Telomerase

Shalmica R. Jackson,<sup>1</sup> Chun-Hong Zhu,<sup>1</sup> Vera Paulson,<sup>1</sup> Linda Watkins,<sup>2,3</sup> Z. Gunnur Dikmen,<sup>1,4</sup> Sergei M. Gryaznov,<sup>5</sup> Woodring E. Wright,<sup>1</sup> and Jerry W. Shay<sup>1,3</sup>

Departments of <sup>1</sup>Cell Biology and <sup>2</sup>Pharmacology and <sup>3</sup>Harold Simmons Comprehensive Cancer Center, University of Texas Southwestern Medical Center, Dallas, Texas; <sup>4</sup>Department of Biochemistry, Faculty of Medicine, University of Hacettepe, Ankara, Turkey; and <sup>5</sup>Geron Corporation, Menlo Park, California

## Abstract

We determined previously that a novel human telomerase RNA (*hTR*) antagonist, GRN163L, inhibited the tumorigenic potential of A549-luciferase (A549-luc) lung cancer cells *in vitro* and *in vivo*. Further studies revealed that A549-luc cells were also morphologically altered by GRN163L. A549-luc cells treated before cell attachment with a single dose of GRN163L only weakly attached to the substrate and remained rounded, whereas control mismatch-treated cells exhibited typical epitheloid appearance and adhesion properties. These morphologic changes were independent of *hTR* expression and telomerase inhibition and were unrelated to telomere length. This effect is dependent on the molecular properties of the lipid moiety, the phosphorothioate backbone, and the presence of triplet-G sequences within the GRN163L structure. Altered adhesion was manifested by a 50% reduction in rapid cellular attachment and a 3-fold decrease in total cell spreading surface area. Administration of a single dose of GRN163L (15 mg/kg) at the time of cell inoculation, using an *in vivo* model of lung cancer metastasis, resulted in significant reductions in tumor burden at days 13, 20, and 27 of tumor progression. Thus, the potent antimetastatic effects of GRN163L may be related, in part, to the antiadhesive effects of this novel cancer therapeutic conferred via specific structural determinants and that these effects are independent of telomerase inhibition or telomere shortening. [Cancer Res 2007;67(3):1121–9]

## Introduction

One challenge in the development of novel anticancer strategies is the identification of new molecular targets. Greater than 90% of all human cancer cells display robust activation of telomerase (1), a unique reverse transcriptase consisting of two major components, the template RNA [human telomerase RNA (*hTR*) or *hTERC*] and the catalytic subunit (*hTERT*; refs. 2–4). In contrast, normal human cells lack telomerase activity, with the exception of male germ-line cells, proliferative cells of renewal tissues (5–7), and perhaps rare cycling primary presenescent human fibroblasts (8). Telomerase activation is necessary for the extensive proliferation and subsequent metastasis of most cancer cells. In the last decade, a variety of methods have been devised to pinpoint telomerase as an exceptional target for cancer therapeutics (9–11). Although some

telomerase inhibitors are entering early-stage clinical trials, there is still much about these inhibitors that are not completely understood.

A new class of oligonucleotide telomerase inhibitors that target the *hTR* component of telomerase has been developed recently (12). GRN163, a N3'→P5' thio-phosphoramidate, causes reversible telomerase inhibition and subsequent telomere shortening in many cell types, including human mammary epithelial cells (13). Importantly, GRN163 is not a typical antisense oligonucleotide targeting mRNA. Because it is a direct enzymatic inhibitor at the *hTR* active site, RNase H is not required and a 50% inhibition of target can lead to telomere dysfunction (14). GRN163-induced telomere erosion also causes the induction of senescence or apoptosis in prostate cancer, multiple myeloma, and non-Hodgkins lymphoma cells as well as a reduction of tumor growth in myeloma and glioblastoma xenograft models (15–17). It has been reported that telomerase has multiple functions besides maintenance of telomeres, which may have some bearing on the observations that GRN163L induces senescence or apoptosis in addition to telomere erosion (18).

As with most anionic oligonucleotides, repeated transfection of GRN163 with cationic lipophilic carriers was required for efficient intracellular uptake because naked oligonucleotides are relatively poorly internalized (19–24). Thus, we synthesized a second generation of GRN163 that contained a 5'-terminal palmitoyl (C16) moiety conjugated to the thio-phosphoramidate backbone of GRN163 and designated it as GRN163L (19). The lipidation of GRN163 greatly increased the intracellular uptake, inhibition of telomerase, rate of telomere shortening, growth inhibition, and apoptosis in human mammary epithelial and hepatoma cell lines (19–21).

Of particular interest was the observation that within only 1 to 2 weeks of treatment with GRN163L, A549 lung cancer and MDA-MB-435 breast cancer cells exhibited reductions in clonal efficiency, loss of anchorage-dependent growth capabilities, and decreased invasiveness (21, 22). These changes in cell behavior were much too rapid to be caused by progressive telomere shortening, which previous researchers have found with the parental GRN163. Indeed, our earlier results indicate that critical telomere shortening in cell culture in the A549 and MDA-MB-435 cell lines required 6 to 8 weeks of continuous treatment with GRN163L (21, 22). However, after 1 day of GRN163L treatment, A549 cells exhibited morphologic alterations, suggesting changes in cellular adhesion (22).

In this report, we characterize the antiadhesive effects of GRN163L *in vitro* and *in vivo*. We show that the morphologic changes induced by GRN163L are independent of *hTR* expression, independent of telomerase holoenzyme inhibition, and unrelated to the telomere length of cancer cells. The rapid morphologic alterations are related to a dysfunction in cell adhesion induced by GRN163L, manifested by a reduction in both the strength of cellular attachment and the total cell spreading surface area. We also report that *in vivo* i.p. administration of a single dose of GRN163L

**Requests for reprints:** Jerry W. Shay, Department of Cell Biology, University of Texas Southwestern Medical Center, 5323 Harry Hines Boulevard, Dallas, TX 75390-9039. Phone: 214-648-3282; Fax: 214-648-8694; E-mail: jerry.shay@utsouthwestern.edu.  
©2007 American Association for Cancer Research.  
doi:10.1158/0008-5472.CAN-06-2306

(15 mg/kg) at the time of cell inoculation results in a reduction in A549-luciferase (A549-luc) lung cancer metastasis. This suggests that the antimetastatic effect of GRN163L on A549 cells may be related, in part, to the anticell adhesive effects of this novel cancer therapeutic. These findings represent an unanticipated mechanism of action for GRN163L, which may open new avenues for therapeutic treatments.

## Materials and Methods

**Cell culture and morphologic analysis.** Human non-small cell lung adenocarcinoma cells (A549) were obtained from American Type Culture Collection (ATCC; Manassas, VA) and grown in XS medium (4:1 DMEM/medium 199 + 10% CCS; HyClone, Logan, UT) at 37°C under 5% CO<sub>2</sub>. A549 cells that express lentivirally delivered luciferase (A549-luc) were generated as described previously (22). BJ (normal skin fibroblasts), SUSM-1 (4-nitroquinoline-immortalized liver fibroblasts), and VA13 (SV40-immortalized lung fibroblasts) were all obtained from ATCC.

For morphologic analyses,  $0 \times 10^5$  to  $3 \times 10^5$  cells in 10 mL medium were seeded into 10-cm<sup>2</sup> culture dishes and 1 μmol/L mismatch or 1 μmol/L GRN163L was added directly to the dish before cell attachment. Phase-contrast micrographs were taken using an inverted Zeiss Axiovert 200M at  $\times 20$  magnification (Carl Zeiss-Thornwood, NY).

**Synthesis of oligodeoxynucleotides.** All oligonucleotides, except the shorter versions of GRN163L, were synthesized as described previously (15). Truncated versions of GRN163L (11, 9, and 7 mer) were purchased from Transgenomic, Inc. (Omaha, NE). The prepared oligonucleotides were solubilized in normal saline and their concentrations were determined by UV spectroscopy.

**Telomerase activity assay.** Telomerase activity from cell extracts was analyzed using the PCR-based telomeric repeat amplification protocol (TRAP) assay (1). Samples were resolved by PAGE and scanned using a Storm 860 PhosphorImager scanner system (Molecular Dynamics, GE Healthcare, Piscataway, NJ). Quantitation and visualization of the TRAP gels were as described (21, 22).

**Generation of adenoviral hTERT-A549-luc cells.** A549-luc cells (70% confluent) were exposed to adenoviral hTERT (AdhTERT; multiplicity of infection of 30) for 16 h in medium without serum. The virus was then removed and complete medium was then added. Transfection frequency was  $\geq 75\%$  after 24 h.

**Immunofluorescence.** A549-luc and A549-luc-AdhTERT cells ( $1 \times 10^4$ /300 μL medium) were seeded into eight-well chamber slides and allowed to attach overnight. Then, the cells were fixed in 4% PAF, permeabilized with 0.1% Triton X-100, and blocked with 0.5% bovine serum albumin (BSA). The slides were incubated with antimouse hTERT antibody (1A4; 5 μg/mL) produced at Geron Corp. (Menlo Park, CA) and rhodamine-conjugated goat anti-mouse IgG (Jackson ImmunoResearch Laboratory, Inc., West Grove, PA), then mounted with Vectoshield + 4',6-diamidino-2-phenylindole (Vector Laboratories, Inc., Burlingame, CA), and viewed using a Zeiss Axiovert 200M microscope. All original pictures were taken using a magnification of  $\times 20$ .

**hTR reverse transcription-PCR.** Total cellular RNA was extracted from cultured cells using RNeasy Mini kit (Qiagen, Valencia, CA) according to the manufacturer's instructions. Reverse transcription-PCR (RT-PCR) was done using a one-step RT-PCR kit (Invitrogen) with hTR primers: 5'-TCTAACCTAACTGAGAAGGGCGTAG-3' (F3B-hTR) and 5'-CCAG-CAGCTGACATTTTTTG-3' (Htr189R; ref. 25). As internal controls for the quantity and quality of the RNA specimens, RT-PCR amplifications targeting transcripts of the housekeeping gene *glyceraldehyde-3-phosphate dehydrogenase* were done in parallel.

**Cell attachment and spreading assays.** Cell attachment and spreading were carried out following the methodology described in *Current Protocols in Cell Biology* (Cell Substrate Adhesion Assays 9.1).<sup>6</sup> Briefly, wells in a

96-well plate (Nalge Nunc, Rochester, NY) were coated overnight at 4°C with Dulbecco's PBS (DPBS) or type I collagen (1–25 μg/mL; BD Biosciences, San Jose, CA). Free collagen was aspirated and wells were blocked with HI-BSA (10 mg/mL) overnight at 4°C. Wells were washed with DPBS. A549-luc cells were trypsinized briefly and detached quickly. Cells ( $1 \times 10^5$ /mL for spreading and  $1 \times 10^6$ /mL for attachment) were resuspended gently in CO<sub>2</sub>-conditioned medium [DMEM-HEPES-10% fetal bovine serum gassed with 5% (v/v) CO<sub>2</sub> for 20–30 min]. Care was taken to guard against cell clumping and aggregation. Cells in conditioned medium were placed in 50 mL tubes in incubators (5% CO<sub>2</sub> at 37°C) uncovered for 10 to 15 min to allow for the recovery from trypsinization and the reexpression of cell surface molecules that mediate cell attachment and spreading. Mismatch or GRN163L was diluted with DPBS and the diluted oligonucleotides were added to the 96-well plate, and then  $5 \times 10^3$  cells for spreading and  $5 \times 10^4$  cells for attachment were added to the wells.

For attachment assays, cells (in triplicate) were incubated with oligonucleotides for 20 min at 37°C. Cells were washed, which removed some weakly adherent cells, and fixed with 5% glutaraldehyde for 20 min at room temperature. The fixed cells were stained with filtered 0.1% crystal violet diluted in 200 mmol/L MES (pH 6) for 1 h at room temperature. The dye was solubilized in 10% acetic acid for 15 min on an orbital shaker. Absorbance was measured at 570 nm using a microtiter plate reader. Data are expressed as relative attachment, which is equivalent to absorbance. For spreading assays, conditioned cells were incubated with test oligonucleotides for 90 min at 37°C. Media were aspirated and cells were fixed directly with 5% glutaraldehyde for 30 min room temperature. Fixative was aspirated and cells were stored at 4°C in CMF-DPBS-Na<sub>3</sub>. Cells were viewed on an inverted phase-contrast microscope at  $\times 63$ , oil using a Zeiss Axiovert 200M. Total cell surface area was quantified with Axio-Vision (Carl Zeiss MicroImaging Thornwood, NY).

**Xenograft mice experiments and bioluminescence *in vivo* imaging of A549-luc cells.** Immunodeficient mice (*nu/nu*; Harlan Sprague Dawley, Inc., Indianapolis, IN) were maintained in pathogen-free conditions within the Animal Research Committee (ARC) at the University of Texas Southwestern Medical Center and treated according to ARC and Animal Care and Use Committee guidelines. Mice were irradiated with 3.5 Gy <sup>137</sup>Cs 18 to 24 h before tail vein injections with A549-luc cells. The cell viability was checked via trypan blue exclusion and  $1 \times 10^6$  cells/200 μL NaCl (0.9%) were injected into the tail vein of four mice per group. Immediately after cell inoculation, mice were given a single dose of either mismatch (15 mg/kg) or GRN163L i.p. Mice were imaged weekly using a novel light emission tomography system as described previously (21, 22). All images were taken for 10 min. Signal intensity was quantified as the sum of all detected photon counts within the region of interest after subtraction of background luminescence using Igor Pro software.

## Results

**Rapid morphologic alterations induced by GRN163L.** A549-luc cells were treated before cell attachment with a single dose of either 1 μmol/L mismatch control oligonucleotide (mismatch) or GRN163L (163L), and cell morphology and telomerase inhibition were assessed after 24, 48, and 72 h of incubation (Fig. 1A). After 24 h, the mismatch-treated cells exhibited a typical epitheloid appearance with properly flattened cytoplasmic extensions and evidence of proliferation, whereas the 163L-treated cells were weakly attached, rounded up, and had thin elongated cytoplasmic extrusions. This altered cellular morphology was persistent after prolonged treatment (Fig. 1A). Telomerase activity was also reduced >90% in A549-luc cells treated with a single dose of 1 μmol/L 163L (Fig. 1B and C). Even after 72 h, the growth rate of the A549 cells was only reduced by 35%, suggesting that GRN 163L is not overtly toxic (data not shown).

**GRN163L-induced altered cell morphology is independent of hTR and telomerase holoenzyme inhibition.** To determine if

<sup>6</sup> www.does.org/masterli/cpcb.html.

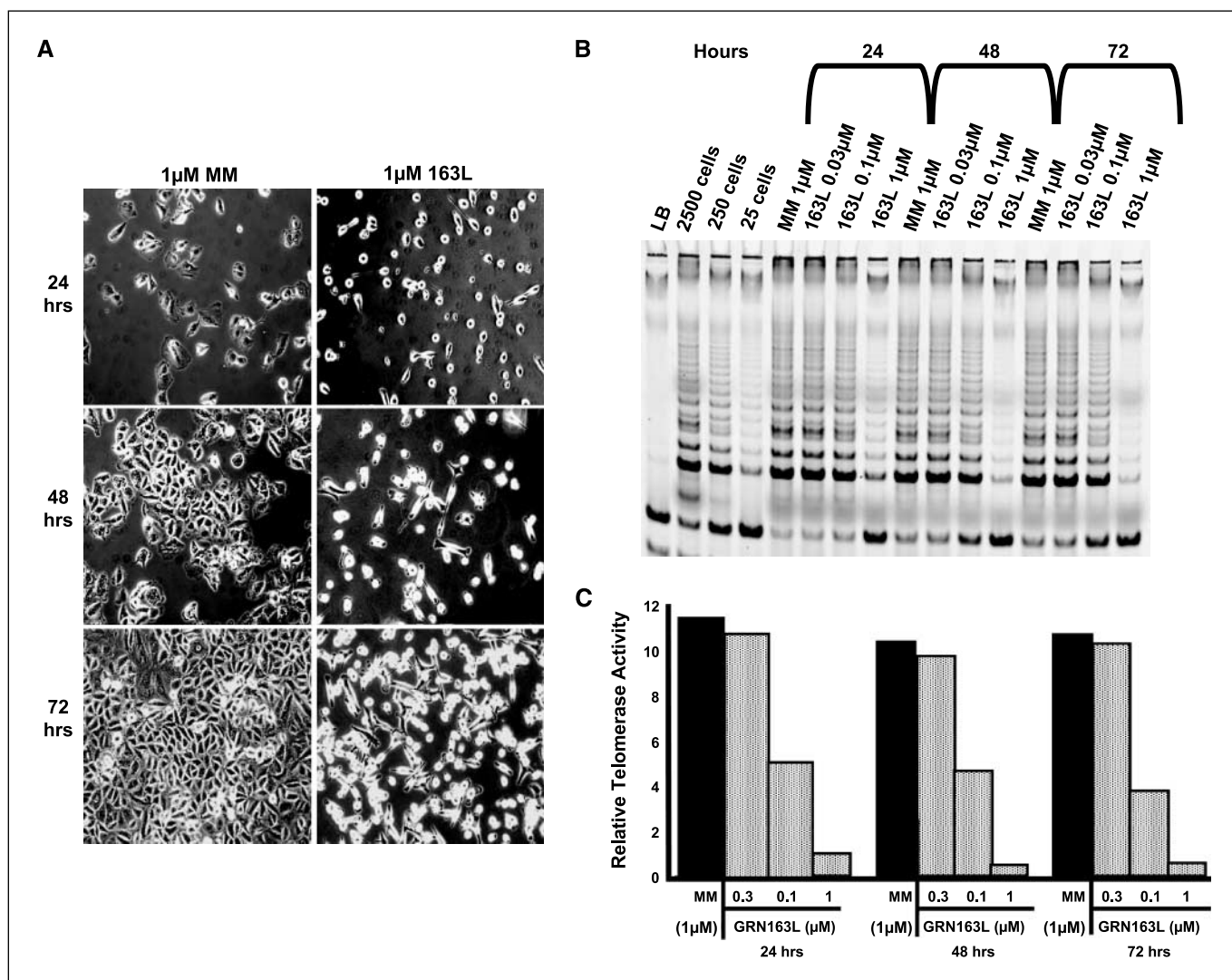


**Figure 1.** Morphologic alterations (A), inhibition of telomerase activity (B), and quantitation (C) in A549-luc lung adenocarcinomas cells induced by GRN163L (163L). A, A549-luc cells ( $1 \times 10^5$ ) were treated with either 1  $\mu$ mol/L mismatch (MM) or 163L before cell attachment, and phase-contrast photomicrographs ( $\times 20$ ) were taken after 24, 48, or 72 h of treatment. Similar results were obtained in at least five independent experiments. B, TRAP analysis of telomerase activity (TRAP activity) of A549-luc cells ( $1 \times 10^5$ ) treated before cell attachment with either mismatch or different doses of 163L. Lane 1, negative control [lysis buffer (LB)]; lanes 2 to 4, positive controls [H1299 cells (2,500, 250, and 25 cells)]; lanes 5 to 8, 24 h of treatment of mismatch or 163L; lanes 9 to 12, 48 h of treatment of mismatch or 163L; lanes 13 to 16, 72 h of treatment of mismatch or 163L. C, quantification of TRAP activity gel. Similar results were obtained in a separate independent experiment.

the altered cellular phenotype induced by 163L was mediated via hTR, hTR-negative cells were examined. Both the SUSM-1-immortalized liver fibroblasts and the VA13 lung fibrosarcoma cells (Fig. 2A) were altered morphologically by 163L, whereas normal BJ foreskin fibroblasts, which express low-to-moderate levels of hTR (data not shown), were not affected by 163L. This provides evidence that hTR per se is not involved in the altered morphology induced by GRN163L. Figure 2B shows the RT-PCR confirmation of the lack of hTR expression in SUSM-1 and VA13 cells. VA13 cells expressing an exogenous hTR (VA13hTR) were used as a positive control.

Truncated versions of 163L that have less of a telomerase inhibitory effect were synthesized in efforts to determine if telomerase inhibition and/or oligonucleotide length was essential for the alteration of A549 cell morphology (Table 1). A549-luc cells were treated with a single dose of mismatch or 13-, 11-, 9-, and 7-mer GRN163L-derived oligonucleotides at the time of cell

attachment. All three of the shorter oligomers (11, 9, and 7 mer) caused the altered cell phenotype within 24 h (7-mer; Fig. 2C) to the same extent as the full-length 13 mer. As expected, the truncated oligomers (11, 9, and 7 mer) had decreasing abilities to inhibit telomerase activity when compared with the full-length 13-mer 163L (Fig. 2D). The 7-mer minimally inhibited telomerase activity (Fig. 2D) yet induced the same magnitude of antiadhesive effects as 163L (Fig. 2C). These data suggested that GRN163L has two independent mechanisms of action in the A549 cells: one well-characterized effect on telomerase inhibition, directly mediated by its interaction with the hTR, and another novel anti-cell adhesive mechanism, which is independent of hTR expression and telomerase inhibition.

**Short telomeres are unlikely to be related to changes in cell shape stimulated by GRN163L.** Inhibition of telomerase may lead to the erosion of a few critically short telomeres causing telomere end-end fusions and subsequent mitotic catastrophe, culminating



in widespread intracellular destruction. We tested the hypothesis that the anti-cell adhesive effect of GRN163L may be due to catastrophic telomere deletion events that occur as a result of telomerase inhibition. Because A549 cells have heterogeneous telomeres (23), we transiently elongated telomeres via infection with AdhTERT (Fig. 3). Because adenoviral vectors are not integrated into the genome, AdhTERT only transiently elongates the shortest parental telomeres, and after approximately 2 to 3 weeks, its expression is undetectable. Thus, we transiently elongated telomeres, waited 2 to 3 weeks (14–22 population doublings), and then determined if the treatment with GRN163L induced alteration of the cell morphology. Figure 3A shows the immunofluorescence localization of exogenously expressed AdhTERT using a monoclonal antibody (GRN 1A4) that recognizes hTERT. Control A549-luc cells contain too little hTERT to be seen with the GRN 1A4 monoclonal antibody. However, exogenously expressed hTERT was detected in 40% of A549 cells + AdhTERT after 6 days of infection. By 16 days of infection, only 10% of AdhTERT cells could be detected, and by 33 days, no A549 cells were immunopositive, indicating that the AdhTERT had become

diluted out during cell propagation. The transient infection with AdhTERT coincided with a 60-fold increase in TRAP activity after 6 days of infection, and by 33 days, TRAP activity had returned to basal levels (Fig. 3B and C). Figure 3D shows that control A549-luc cells treated with a single dose of 1  $\mu\text{mol/L}$  163L at the time of seeding exhibited an altered cell morphology after 24 h of incubation (Figure 3D, top). Similarly, A549-luc cells with adenovirally elongated telomeres remained susceptible to the rapid morphologic changes induced by GRN163L (Figure 3D, middle and bottom). These experiments suggest that critically short telomeres on some chromosomes are not involved in the morphologic changes induced by GRN163L.

**GRN163L-induced altered A549-luc cell adhesion is due to a reduction in cell attachment and an inhibition of cell spreading.** To determine if the rapid morphologic alterations were related to a dysfunction in cell adhesion, A549-luc cells were treated before cell attachment (Fig. 4A, top) or after overnight attachment (Fig. 4A, bottom) with a single dose of either 1  $\mu\text{mol/L}$  mismatch control or GRN163L (Fig. 4A). Interestingly, 163L only alters cell adhesion when the cells were treated before cell attachment. These

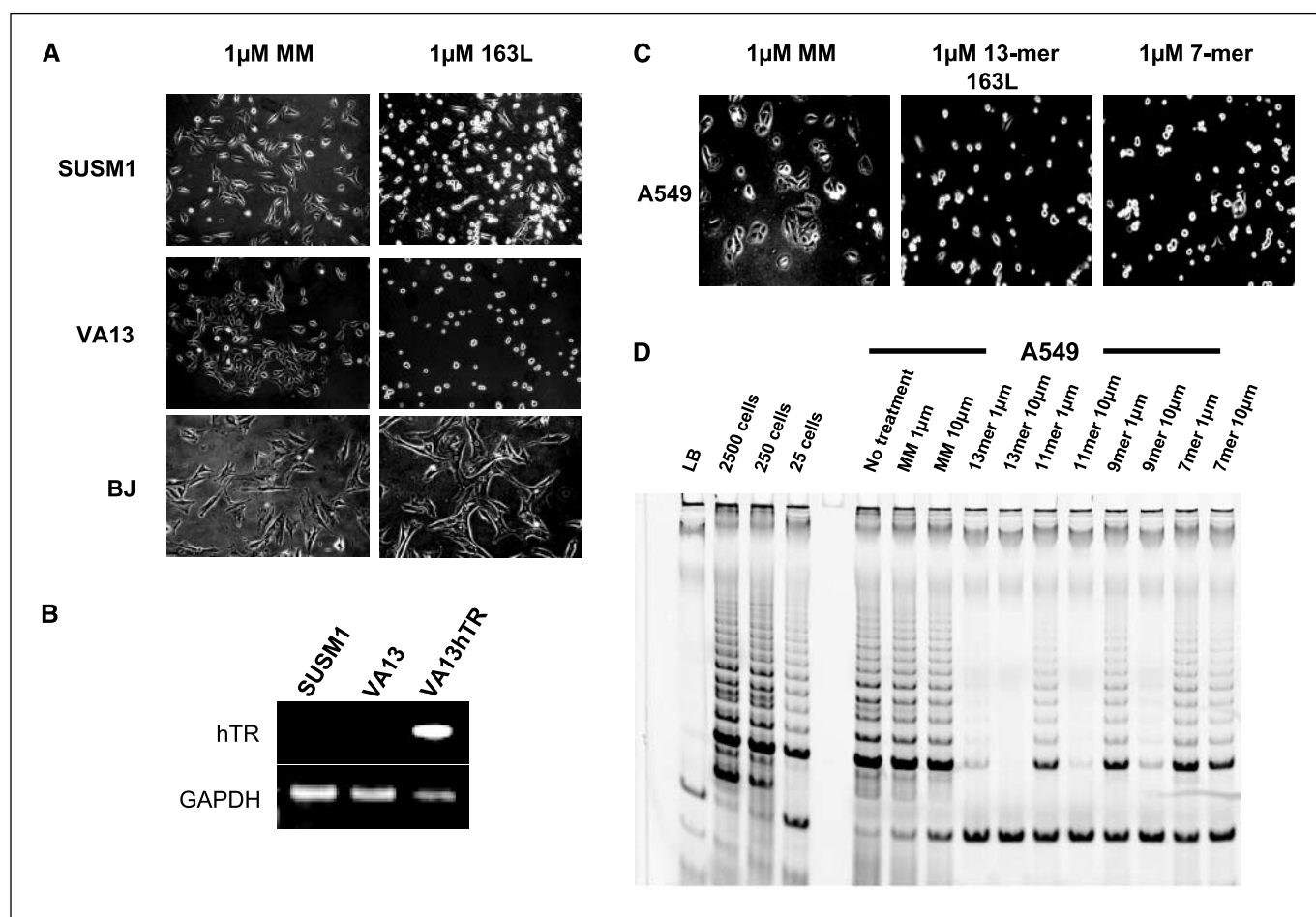


**Figure 2.** GRN163L-induced altered cell morphology is independent of hTR (A and B) and telomerase activity (C and D). A, SUSM-1 and VA13 (both hTR negative) and normal BJ cells were treated before cell attachment with either 1  $\mu\text{mol/L}$  mismatch or 163L, and phase-contrast photomicrographs ( $\times 20$ ) were taken after 24 h of treatment. Similar results were obtained in at least three independent experiments. B, RT-PCR analysis of hTR levels in SUSM-1, VA13, and VA13hTR cells. C, A549-luc cells were treated before cell attachment with either 1  $\mu\text{mol/L}$  mismatch, 13-mer 163L, or 7-mer, and phase-contrast photomicrographs ( $\times 20$ ) were taken after 24 h of treatment. Similar results were obtained in three independent experiments. D, 24 h of TRAP analysis of A549-luc cells treated before cell attachment with 1 or 10  $\mu\text{mol/L}$  of either 13-mer mismatch or truncated oligomers of 163L, respectively. Lane 1, negative control (lysis buffer); lanes 2 to 4, positive controls [H1299 cells (2,500, 250, and 25 cells)]; lane 5, no treatment; lanes 6 and 7, 13-mer mismatch; lanes 8 and 9, 13-mer 163L; lanes 10 and 11, 11-mer 163L; lanes 12 and 13, 9-mer 163L; lanes 14 and 15, 7-mer 163L. Similar results were obtained in a separate independent experiment.

findings suggested that an aspect of cell adhesion was involved in this antiadhesive phenomenon induced by GRN163L.

Using a colorimetric assay to determine cell attachment efficiency, Fig. 4B (left) shows that A549-luc cells treated before cell attachment with a single dose of 1  $\mu\text{mol/L}$  GRN163L (163L) exhibit a 50% reduction in the ability to attach firmly to plastic substrata after 20 min when compared with cells treated with 1  $\mu\text{mol/L}$  mismatch control. Interestingly, cells that were treated preattachment, but were seeded into wells coated with type I collagen (1–25  $\mu\text{g/mL}$ ), did not exhibit any differences in attachment strength efficiency when compared with mismatch control-treated cells. Thus, type I collagen blocks the GRN163L-induced rounding that reduced the strength of attachment. Importantly, A549-luc cells, allowed to attach to the plastic substrata for 1 h, were resistant to the antiadhesive effect of 163L (Fig. 4B, right).

The alteration in cell adhesion in the 163L-treated cells, attributed above to an inhibition of cell spreading, is documented in Fig. 4C. A549-luc cells treated before cell attachment (preattachment panels) with a single dose of 1  $\mu\text{mol/L}$  GRN163L have incomplete cytoplasmic protrusions coupled with retarded cell flattening after 90 min of incubation, whereas cells treated with 1  $\mu\text{mol/L}$  mismatch control appear well spread with numerous lamellipodia. Cells that were treated preattachment, but were seeded into wells coated with type I collagen (25  $\mu\text{g/mL}$ ), did not exhibit any differences in the ability to spread and flatten out when compared with mismatch control-treated cells. Quantitatively (Fig. 4D), the 57% reduction in total cell surface area of 163L compared with mismatch-treated cells was abolished in collagen-coated wells (Fig. 4B and D). Thus, type I collagen blocks the GRN163L-induced reduction of cell spreading. Importantly, A549-luc cells that were allowed to attach to the plastic substrata for 1 h were less resistant to 163L because there was only a 22% reduction in cell spreading between the mismatch- and 163L-treated cells (Fig. 4C and D, right).

**Determination of the key molecular components of GRN163L which confer the antiadhesive effect.** To dissect the important antiadhesive features of GRN163L, we designed and tested several other oligonucleotides that were similar in structure but contain specific modifications in the lipid moiety, backbone chemistry, or G-rich motif. Data shown in Table 1 were collected using 1  $\mu\text{mol/L}$  of the oligonucleotides added before plating the cells in plates. Altered adhesion strength (rounding) was determined after 24 h and TRAP inhibition was measured 72 h after oligonucleotide addition.

We predicted that the most important structural component involved in the antiadhesive effect of 163L was the lipidation of the compound because lipidation plays a key role for bioavailability. We observed that the unlipidated parental GRN163 does not alter cell adhesion (Table 1). These data indicate that the potential molecular target may be intracellular. In addition, if the palmitoyl group is substituted for lipids with different structures, such as “teflon” or cholesterol, cell adhesion is reduced because there were inactive at 1  $\mu\text{mol/L}$  but showed effects at 10  $\mu\text{mol/L}$  (data not shown).

We also hypothesized that the nitrogen-phosphorous-sulfur-containing backbone chemistry (NPS linkage) might be important in the anti-cell adhesion induced by 163L. Our data show that oligonucleotides that have alternative backbone chemistries (oligonucleotides 1 and 2; i.e., phosphoramidate oligonucleotides) did not alter cell adhesion, suggesting that the thio-containing backbone chemistry in 163L is an important factor in impeding cell adhesion.

Because the mismatch control differs from 163L only by the lack of three contiguous guanine residues, it seemed that this motif might also be necessary for the altered cell adhesion phenotype. The data collected using the truncated versions of 163L (11, 9, and 7 mer), which retain the triple-G motif, are consistent with this concept. All of these shortened derivatives of 163L alter cell adhesion to the same extent as the full-length 163L-13mer. This

**Table 1.** Summary of *in vitro* experiments testing various modifications of oligomer chemistry on A549-luc TRAP activity (72 h) and cell adhesion alteration (24 h)

Oligonucleotide	Sequence	Lipidation	Backbone chemistry	GGG motif	TRAP inhibition	Adhesion alteration
Mismatch	5'-Palm-TAGGTGTAAGCAA-3'	Palmitoyl	NPS	No	No	No
163L-13 mer	5'-Palm-TAGGGTTAGACAA-3'	Palmitoyl	NPS	Yes	Yes	Yes
163	5'-TAGGGTTAGACAA-3'	None	NPS	Yes	No	No
163L-11 mer	5'-Palm-GTTAGGGTTAG-3'	Palmitoyl	NPS	Yes	Yes	Yes
163L-9 mer	5'-Palm-GGGTTAGAC-3'	Palmitoyl	NPS	Yes	Yes	Yes
163L-7 mer	5'-Palm-GGGTTAG-3'	Palmitoyl	NPS	Yes	Moderate	Yes
163-teflon	5'-“Teflon”-TAGGGTTAGACAA-3'	Teflon	NPS	Yes	Moderate	No
163-cholesterol	5'-Chol-TAGGGTTAGACAA-3'	Cholesterol	NPS	Yes	Moderate	No
1	5'-Palm-TAGGGTTAGACAA	Palmitoyl	NP	Yes	No	No
2	5'-Oleic-TAGGGTTAGACAA	Oleic	NP	Yes	No	No
3	5'-Palm-CGTACCACGCTCGCTA-3'	Palmitoyl	NPS	No	NA	No
4	5'-Palm-CTAGACTCGGACCCTC-3'	Palmitoyl	NPS	No	NA	No
5	5'-Palm-AACGTTGAGGGGCAT-3'	Palmitoyl	NPS	Yes	No	Yes
6	5'-Palm-AACGAGTTGGGGCAT-3'	Palmitoyl	NPS	Yes	No	Yes

NOTE: Column 1, oligonucleotide designation; column 2, linear sequence; column 3, lipid modifications; column 4, backbone chemistry; column 5, G-rich motif:  $\geq 3$  sequential guanine residues; column 6, 72 h of TRAP inhibition with 1  $\mu\text{mol/L}$  oligonucleotide; column 7, adhesion alteration: assessed by morphologic analysis of cells treated before cell attachment with 1  $\mu\text{mol/L}$  oligonucleotide after 24 h of incubation.

Abbreviations: NP, phosphoramidate; NPS, thio-phosphoramidate.

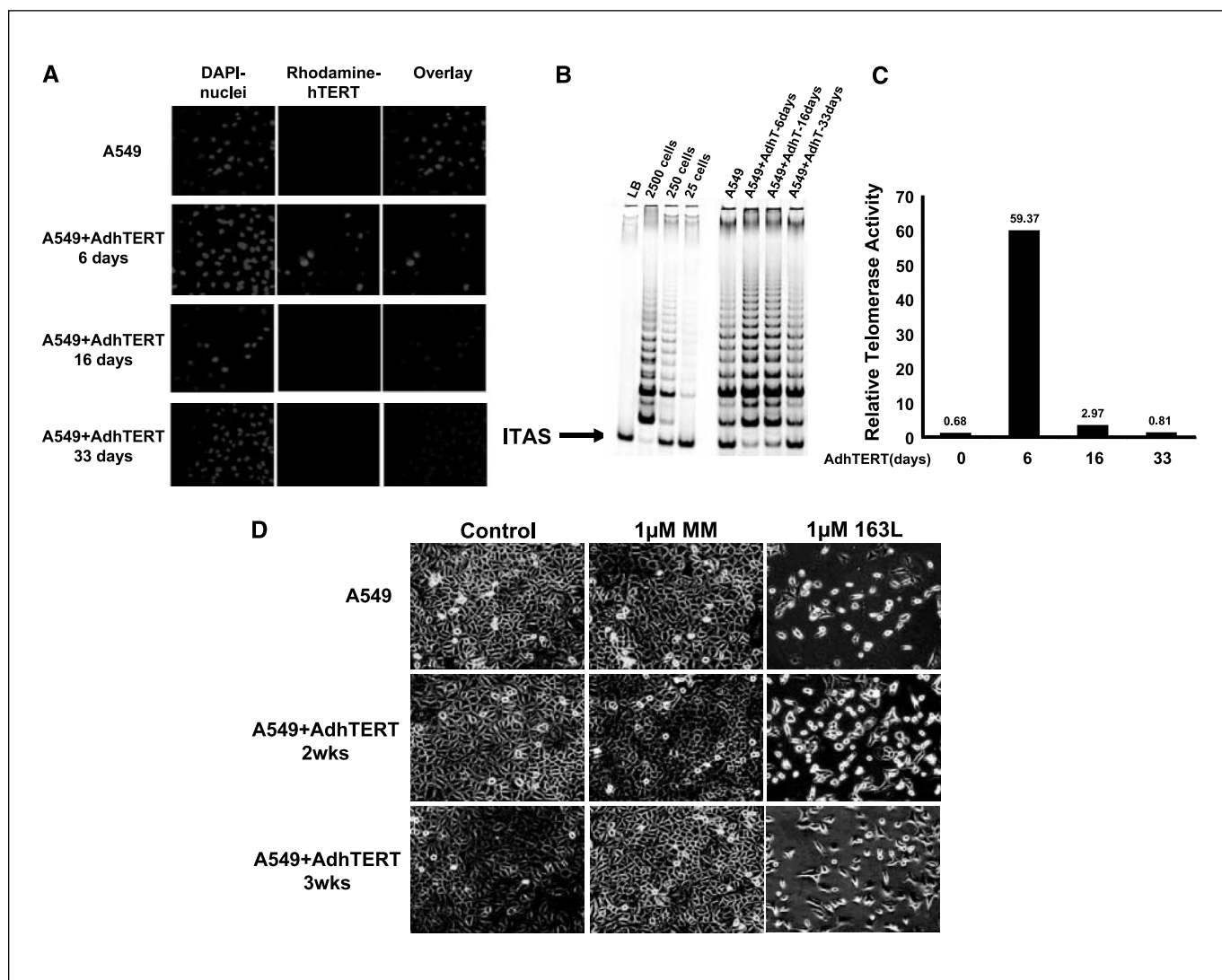


**Figure 3.** Telomere length independency during GRN163L-induced altered A549-luc cell morphology. *A*, immunofluorescent localization of rhodamine-labeled AdhTERT in A549-luc cells after 6, 16, and 33 days of infection. *B*, TRAP analysis of A549-luc cells infected transiently with AdhTERT. *Lane 1*, negative control (lysis buffer); *lanes 2 to 4*, positive controls [H1299 cells (2,500, 250, and 25 cells)]; *lane 5*, A549-luc; *lane 6*, A549-luc+AdhTERT-6 days; *lane 7*, A549-luc+AdhTERT-16 days; *lane 8*, A549-luc+AdhTERT-33 days. *C*, quantification of TRAP activity gel. *D*, A549-luc and A549-luc AdhTERT 2 and 3 weeks postinfection were treated before cell attachment with either 1 μmol/L mismatch or 163L, and phase-contrast photomicrographs ( $\times 20$ ) were taken after 24 h of treatment. Similar results were obtained in a separate independent experiment.

hypothesis is further supported by the fact that oligonucleotides 3 and 4, which lack the triple-G motif, do not alter A549 cell adhesion.

Thus, it seems that the combination of lipophilicity conferred by the palmitic group, the thio-containing backbone chemistry, and the triple-G motif all contribute to making GRN163L an antiadhesive agent. This is best exemplified by oligonucleotides 5 and 6, which contain the three aforementioned molecular determinants and subsequently alter adhesion with no effect on telomerase inhibition; further distinguishing the antiadhesive mechanisms from the telomerase inhibitory effects.

**A single dose of GRN163L given *in vivo* reduces A549-luc cell metastasis to the lung.** A human xenograft model of lung cancer metastasis was used to determine the effect of a single i.p. dose of GRN163L (15 mg/kg) given at the time of i.v. A549-luc lung cancer cell inoculation in athymic nude mice. We found that a single dose of GRN163L (15 mg/kg) resulted in a 92%, 76%, and 53%

reduction in tumor load at days 13, 20, and 27, as determined by bioluminescent imaging (of luciferase-expressing A549 cells) of GRN163L versus mismatch-treated (15 mg/kg) controls (Fig. 5). Because reductions in A549-luc cell attachment and spreading were found *in vitro* (Fig. 4), one interpretation of these findings is that the antiadhesive effects of GRN163L may be related, at least in part, to the reductions in lung tumor burden found *in vivo* in this experimental model of metastasis.

## Discussion

Targeted cancer therapeutics are being developed to be more effective and to alleviate the toxic side effects typically elicited by conventional chemotherapeutics. We have developed a new generation of oligonucleotide analogues, lipid-conjugated N3'→P5' thio-phosphoramidate GRN163L, which is a promising anticancer compound (19–24, 26). We have shown previously that this hTR



antagonist efficiently inhibits telomerase, which culminates in a reduction of several transformed and metastatic phenotypes *in vitro* and *in vivo* (19, 21, 22). The ability of GRN163L to act as an anticancer agent, before this report, was believed to be mediated by inhibiting telomerase via direct interaction with the hTR. The results from our present study show a previously uncharacterized antiadhesive effect of GRN163L, which may represent a novel antimetastatic mechanism of action for this compound. Most importantly, we hypothesize that the reduction in A549 lung metastases in GRN163L-treated mice is at least a partial *in vivo* manifestation of the decreased adhesiveness of the A549 cells that we observe *in vitro*.

Furthermore, these rapid morphologic changes induced by GRN163L were independent of its known telomerase inhibitory effect via hTR antagonism. We used two different ALT (telomerase independent) cell lines (SUSM-1 and VA13) that completely lack hTR RNA expression to show that even in the total absence of hTR expression, GRN163L still alters cell morphology (Fig. 2A). This

observation also suggests that the anti-cell adhesive effects of GRN163L may be effective against ALT tumors.

We rationalized that the phenotypic changes in morphology induced by GRN163L were a result of altered cell adhesion. Cell adhesion can be viewed as an intricately orchestrated two-step process (i.e., initial attachment to the substratum and subsequent cell spreading). We found that the changes in cell morphology were prevalent only if the A549-luc cells were treated within the first few hours of cell attachment. If cells were allowed to firmly attach to plastic substrata overnight, they were resistant to the reduced cell attachment and spreading induced by GRN163L (Fig. 4).

Several reports suggest that oligonucleotides with other chemistries (e.g., phosphorothioate oligonucleotides, 2-*O*-Me PS RNA) can also act in a sequence-specific manner to alter cell adhesion due to their protein interactive capabilities (27–30). Phosphorothioates have a sulfur-for-oxygen atom substitution at the backbone phosphorous, which is similar in structure to the novel N3'→P5' *thio*-phosphoramidate oligonucleotide analogue GRN163L

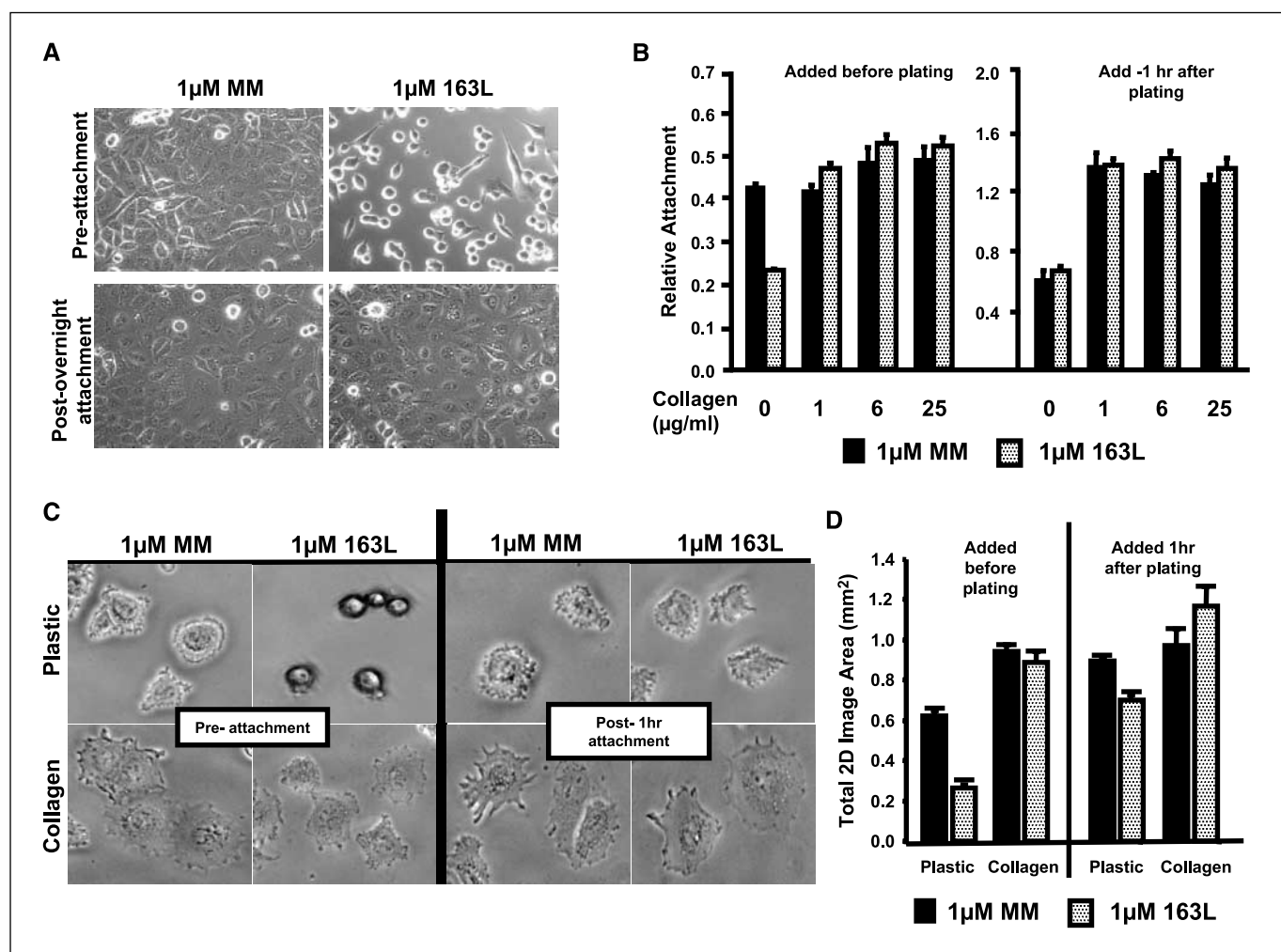


**Figure 4.** GRN163L-induced alteration of A549-luc cell attachment and spreading. *A*, A549-luc cells were treated before cell attachment (*top*) or after overnight attachment (*bottom*) with either 1 μmol/L mismatch or GRN163L, and phase-contrast photomicrographs (×20) were taken after 24 h of treatment. Similar results were obtained in at least five independent experiments. *B*, attachment assay quantitation of A549-luc cells plated on plastic (0 μg/mL) or type I collagen (1, 6, or 25 μg/mL). Cells were treated for 20 min with either 1 μmol/L mismatch or GRN163L before cell attachment (*left*) or for 20 min after 1 h of attachment (*right*). Similar results were obtained in at least three independent experiments. *C*, spreading assay photomicrographs of A549-luc cells plated on plastic or type I collagen (25 μg/mL). Cells were treated for 90 min with either 1 μmol/L mismatch or GRN163L before cell attachment (*left*) or for 90 min after 1 h attachment (*right*). Similar results were obtained in at least three independent experiments. *D*, quantitation of the results of (*C*).

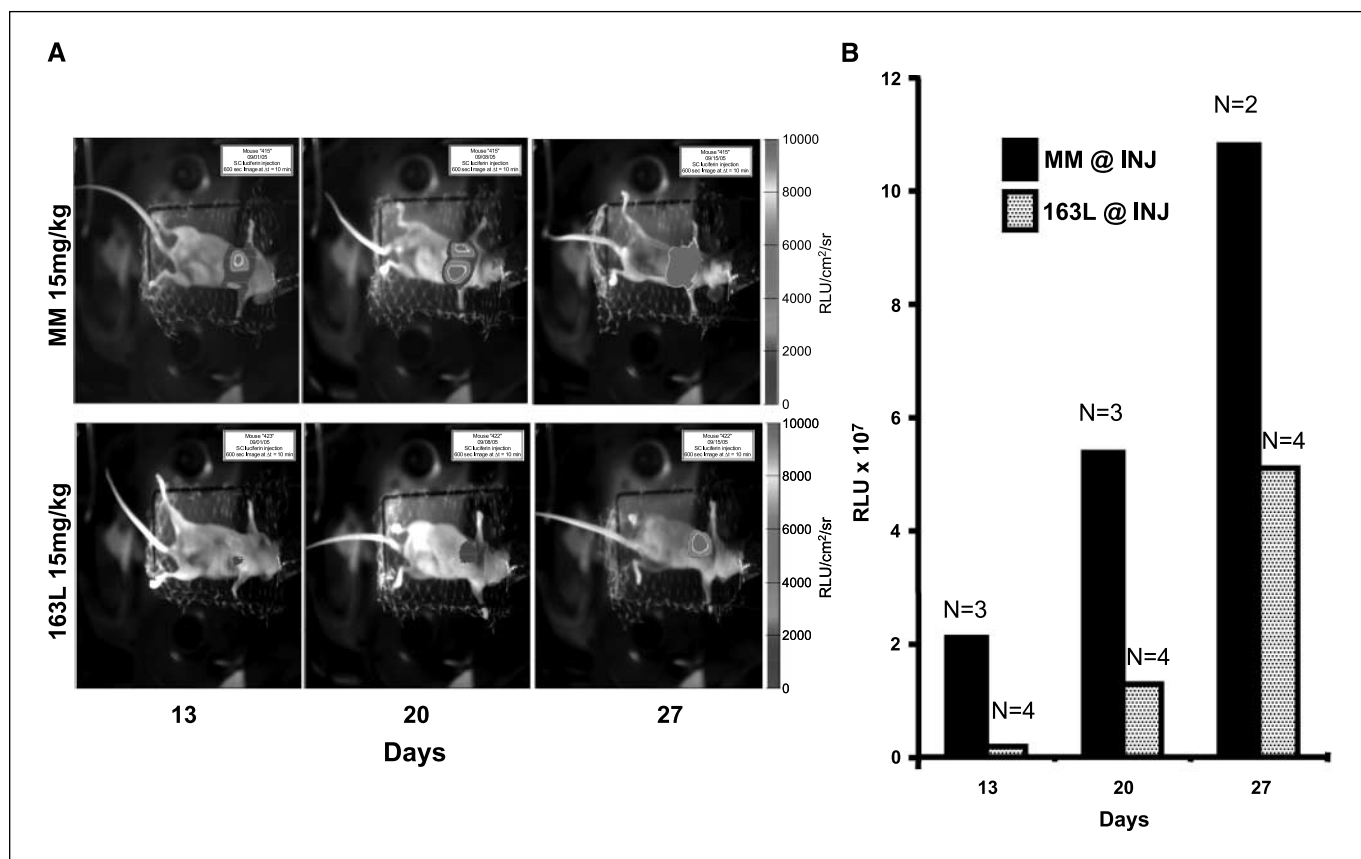


**Figure 5.** Antimetastatic effect of GRN163L on A549-luc ( $1 \times 10^6$ ) *in vivo* (A) and quantitation (B). A, A549-Luc cells were injected via the tail vein into immunodeficient mice. The animals were given a single dose of either mismatch (15 mg/kg) or 163L (15 mg/kg) i.p. at the time of cell inoculation. Bioluminescent images (BLI) of the luciferase-expressing A549 cells were recorded at days 13, 20, and 27 of tumor progression. B, average BLI signals. Similar results were obtained in three independent experiments.

used in this study. GRN163L is a “hybrid” between phosphorothioates and phosphoramidate oligonucleotides because it contains a bridging nitrogen atom included in the backbone, which greatly enhances its hydrolytic stability *in vitro*. Indeed, when oligonucleotide N3'→P5' thio-phosphoramidates were first developed, the chemistry was designed to combine the attractive pharmacokinetic properties of the phosphorothioate protein interactive capabilities with the high RNA binding affinity of the phosphoramidates (12).

The ability of phosphorothioates to bind proteins is not completely understood; however, others have proposed two mechanisms to address the ability of various DNA oligonucleotides to bind to proteins. The first idea is that these highly sulfonated polyanionic molecules can bind in a sequence and length dependent or independent manner with numerous proteins that play key roles in cell adhesion, such as fibronectin, basic fibroblast growth factor, soluble CD4, HIV gp120, laminin, and several protein kinase C isoforms (29, 30). These DNA oligonucleotide-protein interactions are believed to occur via simple ionic and, possibly, covalent chemical bonding resulting from the attraction of the highly electronegative phosphorothioates to basic residues within the proteins in question (24). Our current data neither support nor negate this concept because we observed that oligonucleotides that lack the sulfur moiety in the backbone failed to alter cell adhesion, but the presence of the thio-containing backbone alone is not sufficient to alter cell adhesion (Table 1). It is noteworthy to

mention that the unlipidated GRN163 did not alter adhesion in the same context as GRN163L, suggesting that lipidation and subsequent intracellular localization is important.

The second mechanism through which DNA oligonucleotides bind to proteins may be related to the contiguous deoxyguanosine residues within the sequence because it has been reported that antisense oligonucleotides that have four or more sequential deoxyguanosines can exert an unusual avidity for proteins (27–30). It has also been proposed that G-rich oligonucleotides can form quadruple helices that interact with proteins; however, the mechanisms have not been extensively studied (26). Although it has been shown that G-rich constructs make better anti-cell adhesives, the G-quartet motif seemed necessary but not sufficient to produce an antiadhesive effect: a sequence of three or more deoxyguanosine residues is required to alter cell adhesion (Table 1), but only if palmitic or oleic groups are present.

Interestingly, GRN163L-treated cells seeded into wells coated with type I collagen (1–25  $\mu\text{g}/\text{mL}$ ) did not exhibit any differences in morphologic appearance, attachment efficiency, or cellular spreading when compared with mismatch-treated cells (Fig. 4). Similar results have also been reported for other compounds, such as fibronectin- and laminin-coated dishes. It was reported that a phosphorothioate antisense and sense oligonucleotide directed toward RelA inhibit the adhesion and spreading of K-Balb, MCF-7, and DU-145 cells (30). However, when these cells are seeded onto plates coated with fibronectin or laminin, the antiadhesive effects



of the RelA oligonucleotides were abolished. These researchers also found that type IV collagen or vitronectin had no effect on the antiadhesive effect of the phosphorothioate oligonucleotide. According to the present study findings, type I collagen may interact with GRN163L or provide an alternative spreading surface that substitutes for these blocked by GRN163L, at least *ex vivo* (Fig. 4B–D).

We also show that a single i.p. dose of GRN163L (15 mg/kg) can result in a reduction in the colonization of A549-luc cells into the lung (Fig. 5). This addresses the *in vivo* relevance of the present findings. We hypothesize that the ability of GRN163L to decrease cell attachment and spreading *in vitro* is recapitulated *in vivo* via a reduction in tumor cell seeding and also by a diminished tumor burden in experimental nude mouse models. Because GRN163L recently entered phase I/II clinical trials, it may be beneficial to take advantage of its antiadhesive action by administering the drug at the time of tumor biopsy or tumor-reductive surgery. It has been suggested that fine-needle aspiration may stimulate tumor dissemination through the needle track via the mechanical

exfoliation of cancer cells (31). Thus, a single dose of GRN163L may have a therapeutic effect on any disseminated tumor cells to prevent the reattachment and recolonization and may possibly prevent malignant spread. Pleural carcinosis has been also reported after the excision of malignant lung tumors (32, 33). Therefore, for minimal residual disease, postcytoreductive surgery, GRN163L may also be efficacious in reducing metastatic seeding from tumor cells.

## Acknowledgments

Received 6/23/2006; revised 11/18/2006; accepted 12/1/2006.

**Grant support:** Lung Cancer Specialized Programs in Research Excellence (SPORE) P50 CA75907, Lung Cancer SPORE postdoctoral fellowship (S.R. Jackson), and NASA-sponsored program project NNJ05HD36G.

The costs of publication of this article were defrayed in part by the payment of page charges. This article must therefore be hereby marked *advertisement* in accordance with 18 U.S.C. Section 1734 solely to indicate this fact.

We thank Gregory Thompson, Michael Wang, Jennifer Costley, and Melissa Thompson for superb technical assistance; Angelina Contero and the Cancer Imaging Group for assistance with animal imaging studies; and Krisztina Pongracz and Daria Zielinska at Geron Corp. for oligonucleotide synthesis.

## References

- Shay JW, Bacchetti S. Survey of telomerase activity in human cancer. *Eur J Cancer* 1997;33:787–91.
- Greider C, Blackburn E. Identification of a specific telomere terminal transferase activity in *Tetrahymena* extracts. *Cell* 1985;43:405–13.
- Lingner J, Cooper J, Cech T. Telomerase and DNA end replication: no longer a lagging strand problem? *Science* 1995;269:1533–4.
- Feng J, Funk W, Wang S, et al. The RNA component of human telomerase. *Science* 1995;269:1236–41.
- Shay J, Wright W. Senescence and immortalization: role of telomeres and telomerase. *Carcinogenesis* 2004; 26:867–74.
- Aisner D, Wright W, Shay J. Telomerase regulation: not just flipping the switch. *Curr Opin Genet Dev* 2002;13: 80–5.
- Forsyth N, Wright W, Shay J. Telomerase and differentiation in multicellular organisms: turn it off, turn it on, and turn it off again. *Differentiation* 2002;69: 188–97.
- Masutomi K, Yu EY, Khurts S, et al. Telomerase maintains telomere structure in normal human cells. *Cell* 2003;114:241–53.
- Gellert G, Jackson S, Dikmen Z, Wright W, Shay J. Telomerase as a therapeutic target in cancer. *Drug Discovery Today: Disease Mechanisms* 2005;2:159–64.
- White L, Wright W, Shay J. Telomerase inhibitors. *Trends Biotechnol* 2001;19:114–20.
- Resler E, Bearss D, Hurley L. Telomere inhibition and telomere disruption as processes for drug targeting. *Annu Rev Pharmacol Toxicol* 2003;43:359–79.
- Gryaznov S, Pongracz K, Matray T, et al. Telomerase inhibitors-oligonucleotide phosphoramidates as potential therapeutic agents. *Nucleosides Nucleotides Nucleic Acids* 2001;20:401–10.
- Herbert B-S, Pongracz K, Shay J, Gryaznov S. Oligonucleotide N3'→P5' phosphoramidates as efficient telomerase inhibitors. *Oncogene* 2002;21:638–42.
- Shay JW, Wright WE. Telomeres in dyskeratosis congenita. *Nat Genet* 2004;36:437–8.
- Asai A, Oshima Y, Yamamoto Y, et al. A novel telomerase template antagonist (GRN163) as a potential anticancer agent. *Cancer Res* 2003;63:3931–9.
- Ozawa T, Gryaznov S, Hu L, et al. Antitumor effects of specific telomerase inhibitor GRN163 in human glioblastoma xenografts. *Neuro-Oncol* 2004;6:218–26.
- Wang ES, Wu K, Chin AC, et al. Telomerase inhibition with an oligonucleotide telomerase template antagonist: *in vitro* and *in vivo* studies in multiple myeloma and lymphoma. *Blood* 2004;103:258–66.
- Sharma GG, Gupta G, Wang H, et al. hTERT associates with human telomeres and enhances genomic stability and DNA repair. *Oncogene* 2003;22:131–46.
- Herbert B-S, Gellert GC, Hochreiter A, et al. Lipid modification of GRN163, a N3'→P5' thio-phosphoramidate oligonucleotide, enhances the potency of telomerase inhibition. *Oncogene* 2005;24:5262–8.
- Djojicubroto M, Chin A, Go N, et al. Telomerase antagonists GRN163 and GRN163L inhibit tumor growth and increase chemosensitivity of human hepatoma. *Hepatology* 2005;42:1127–36.
- Gellert G, Dikmen Z, Wright W, Gryaznov S, Shay J. Effects of a novel telomerase inhibitor, GRN163L, in human breast cancer. *Breast Cancer Res Treat* 2006;96:73–81.
- Dikmen ZG, Gellert GC, Jackson S, et al. *In vivo* inhibition of lung cancer by GRN163L: a novel human telomerase inhibitor. *Cancer Res* 2005;65:7866–73.
- Perry P, Arnold J, Jenkins T. Telomerase inhibitors for the treatment of cancer: the current perspective. *Expert Opin Investig Drugs* 2001;10:2141–56.
- Chen Z, Koeneman KS, Corey DR. Consequences of telomerase inhibition and combination treatments for the proliferation of cancer cells. *Cancer Res* 2003;63: 5917–25.
- Yi X, Tesmer VM, Savre-Train I, Shay JW, Wright WE. Both transcriptional and posttranscriptional mechanisms regulate human telomerase template RNA levels. *Mol Cell Biol* 1999;19:3989–97.
- Akiyama M, Hideshima T, Shamma MA, et al. Effects of oligonucleotide N3'→P5' thio-phosphoramidate (GRN163) targeting telomerase RNA in human multiple myeloma cells. *Cancer Res* 2003;63:6187–94.
- Dias N, Stein C. Potential roles of antisense oligonucleotides in cancer therapy. The example of Bcl-2 antisense oligonucleotides. *Eur J Pharm Biopharm* 2002;54:263–9.
- Stein C, Cheng Y. Antisense oligonucleotides as therapeutic agents—is the bullet really magical? *Science* 1993;261:1004–12.
- Guvakova MA, Yakubov LA, Vlodavsky I, Tonkinson JL, Stein CA. Phosphorothioate oligodeoxynucleotides bind to basic fibroblast growth factor, inhibit its binding to cell surface receptors, and remove it from low affinity binding sites on extracellular matrix. *J Biol Chem* 1995; 270:2620–7.
- Khaled Z, Benimetskaya L, Zeltser R, et al. Multiple mechanisms may contribute to the cellular anti-adhesive effects of phosphorothioate oligodeoxynucleotides. *Nucleic Acids Res* 1996;24:737–45.
- Sawabata N, Ohta M, Maeda H. Fine-needle aspiration cytologic technique for lung cancer has a high potential of malignant cell spread through the tract. *Chest* 2000;118:936–9.
- Buhr J, Hurtgen M, Kelm C, Schwemmler K. Tumor dissemination after thoracoscopic resection for lung cancer. *J Thorac Cardiovasc Surg* 1995;110:855–6.
- Downey R, McCormack P. Dissemination of malignant tumors after video-assisted thoracic surgery: a report of twenty-one cases. The video-assisted thoracic surgery study group. *J Thorac Cardiovasc Surg* 1996;111:954–60.

# Cancer Research

The Journal of Cancer Research (1916–1930) | The American Journal of Cancer (1931–1940)

## Antiadhesive Effects of GRN163L—An Oligonucleotide N3'→P5' Thio-Phosphoramidate Targeting Telomerase

Shalmica R. Jackson, Chun-Hong Zhu, Vera Paulson, et al.

*Cancer Res* 2007;67:1121-1129.

**Updated version** Access the most recent version of this article at:  
<http://cancerres.aacrjournals.org/content/67/3/1121>

**Cited articles** This article cites 33 articles, 10 of which you can access for free at:  
<http://cancerres.aacrjournals.org/content/67/3/1121.full#ref-list-1>

**Citing articles** This article has been cited by 6 HighWire-hosted articles. Access the articles at:  
<http://cancerres.aacrjournals.org/content/67/3/1121.full#related-urls>

**E-mail alerts** [Sign up to receive free email-alerts](#) related to this article or journal.

**Reprints and Subscriptions** To order reprints of this article or to subscribe to the journal, contact the AACR Publications Department at [pubs@aacr.org](mailto:pubs@aacr.org).

**Permissions** To request permission to re-use all or part of this article, use this link  
<http://cancerres.aacrjournals.org/content/67/3/1121>.  
Click on "Request Permissions" which will take you to the Copyright Clearance Center's (CCC) Rightslink site.